The influence of defects on the transport properties of $AgSbPb_{18}Te_{20}$ prepared at high pressure and high temperature

2007 J. Phys.: Condens. Matter 19 425219

(http://iopscience.iop.org/0953-8984/19/42/425219)

IOP PUBLISHING JOURNAL OF PHYSICS: CONDENSED MATTER

J. Phys.: Condens. Matter **19** (2007) 425219 (9pp) doi:10.1088/0953-8984/19/42/425219

The influence of defects on the transport properties of $AgSbPb_{18}Te_{20}$ prepared at high pressure and high temperature

Yi Wang, Pinwen Zhu, Hujun Jiao, Haiyong Chen, Yanming Ma, Yingli Niu, Yingai Li, Lijun Zhang, Tiechen Zhang, Chunxiao Gao and Guangtian Zou[1]

National Lab of Superhard Materials, Jilin University, Changchun 130012, People's Republic of China

E-mail: gtzou@jlu.edu.cn

Received 3 August 2007
Published 18 September 2007
Online at stacks.iop.org/JPhysCM/19/425219

Abstract

We synthesized polycrystal $AgSbPb_{18}Te_{20}$ by using the method of high pressure and high temperature, and found that the defects produced by high pressure and high temperature caused the changes of transport properties. X-ray diffraction patterns showed that the cell parameters did not change obviously with synthesis at high pressure, apart from a small fluctuation. The electrical resistivity first increased, and then decreased to one quarter of the original value, as the synthesis pressure changed from low to high. The Seebeck coefficient decreased with the increase of synthesis pressure, and then changed from positive to negative. High pressure and high temperature could cause $AgSbPb_{18}Te_{20}$ to change from a p-type to n-type semiconductor, increase the carrier concentration at maximum by two orders of magnitude, and shift the infrared absorption edge to a higher energy range. All of these phenomena were regarded as showing that high pressure and high temperature favored the formation of certain defects which could change the band structure and thereby change the transport properties.

1. Introduction

High pressure can have a very large effect on the chemical and physical properties of matter. It can help us to access to a wide range of new compounds and unusual states of matter. For thermoelectric materials, pressure has played an important role in tuning bulk thermoelectric materials' band structures and their transport properties [1]. Some findings [2–4] have been reported that high pressure could result in a significant modification in the thermoelectric

[1] Author to whom any correspondence should be addressed.

0953-8984/07/425219+09$30.00

properties of certain materials, such as $BaBiTe_3$, $Sb_{1.5}Bi_{0.5}Te_3$, and $Nd_xCe_{3-x}Pt_3Sb_4$. In particular, a remarkable kind of hysteresis of Seebeck coefficients was observed after unloading the pressure, and the hysteresis only appeared when the pressure was loaded to some high level. These hysteresis effects have attracted much attention since some quantities that are important for applications, such as the power factor, are significantly influenced. Although the origin of the hysteresis is not clear yet, the formation of defects [2, 3] induced by high pressure might provide an explanation, and this possibility is the motivation of the present work. In this paper we investigate the influence of defects produced by high pressure and high temperature (HPHT) on the transport properties and the dependence of the influence on the synthesis pressure.

Defects in semiconductors are known to profoundly alter their electronic structure near the band gap and to control their transport properties. Electronic properties of semiconductors in general, and thermoelectric behavior in particular, are dominated by defects. Some results concerning the relation between transport properties and defects have been reported [5–9]. In recent years the novel quaternary compounds [10] $AgSbPb_{2n-2}Te_{2n}$ ($n = 9, 10$) have attracted considerable attention because of their large thermoelectric figure of merit. It is believed that the modification of the electronic states near the band gap region of PbTe caused by nanostructures formed by Ag and Sb ions in the PbTe matrix is responsible for the observed superior thermoelectric properties of this kind of compound [10–12]. The electronic structures of the $AgSbPb_{2n-2}Te_{2n}$ systems are very sensitive to microstructures composed of Ag, Sb, Pb, and Te, and different microstructures cause $AgSbPb_{2n-2}Te_{2n}$ to change from a semiconductor to a semimetal [13]. So because of the sensitivity of its electronic structure to the microstructures, we chose $AgSbPb_{18}Te_{20}$ as the target for HPHT research.

The early results revealed the hysteresis by using an *in situ* diamond anvil cell (DAC) [2–4]. The sample in the DAC is very small, so it is difficult to move the sample to ambient pressure to do further tests on the effect of stress. In order to eliminate this flaw, we used the HPHT method [14–17] to produce our samples. Our high-pressure apparatus is a cubic anvil cell with a big sample chamber of 10 mm in diameter and 5 mm in length, and the large chamber guarantees that our sample has large dimensions, in order to facilitate the measurements. Our samples were quenched to the ambient pressure and room temperature, and they were not crushed after being synthesized under HPHT. So, we can test more physical quantities of samples synthesized by HPHT at ambient pressure conditions than of samples pressed by a DAC. Quenching is very important in our HPHT synthesis, as it is helpful to produce and keep as many defects produced under high pressure as possible.

2. Experimental details

The sintered polycrystalline samples of $AgSbPb_{18}Te_{20}$ under different pressure were prepared as follows. High-purity (99.999%) Ag, Sb, Pb, and Te powders with 1:1:18:20(at.%) ratio were uniformly mixed in an agate mortar under argon atmosphere, and shaped by a press into a cylinder of 10 mm in diameter and 5 mm in length. To investigate the effect of high temperature and high pressure, two kinds of $AgSbPb_{18}Te_{20}$ compound were prepared by different methods. One was sintered at ambient pressure in a sealed vacuum quartz ampoule (5×10^{-3} Pa) to 1130 K for 4 h and was cooled at the rate of 10 K h^{-1}. In order to compare with samples containing defects produced by HPHT, we chose slow cooling, thereby avoiding unnecessary defects produced by cooling quickly in this kind of sample. The others were synthesized in a cubic anvil high-pressure apparatus under a high temperature of 1270 K and high pressure: 3.6, 4.4, 5.2, and 5.4 GPa. A 10 min experimental run was adopted for all of the samples. After that, the sample was quenched to room temperature, and then the pressure was unloaded. We found that, for HPHT, 1270 K and not 1130 K caused the reaction to finish, so all the samples

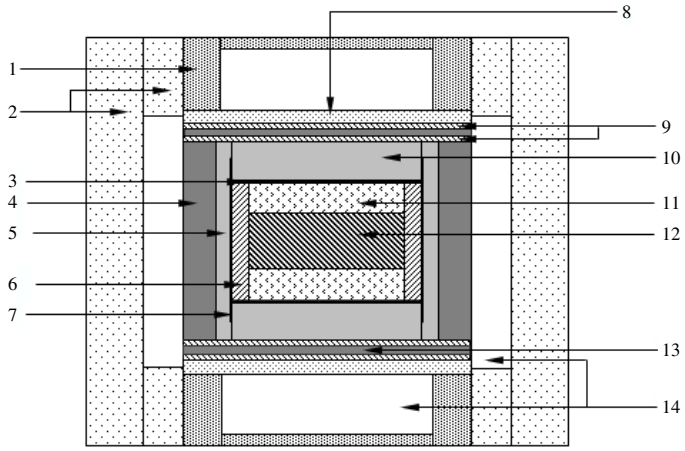

Figure 1. Schematic diagram of the high-pressure sample chamber. 1—steel cap; 2—pyrophyllite; 3—molybdenum plate; 4—graphite heater; 5—pyrophyllite tube; 6—quartz tube; 7—molybdenum foil; 8—iron plate; 9—copper plate; 10—pyrophyllite plate; 11—quartz plate; 12—sample; 13—graphite heater; 14—dolomite.

were synthesized at 1270 K under different high pressure. A schematic diagram of the high-pressure sample chamber is shown in figure 1. The pressure was estimated by the oil press load, which was calibrated by the pressure-induced phase transitions of bismuth, thallium and barium metals. The synthetic temperatures of our samples were estimated by the relationship between input heater power and temperature, here measured by a platinum–rhodium thermocouple. We did not synthesize high-pressure samples below 3.6 GPa, because high temperature and low pressure is dangerous for a high-pressure apparatus. After these two kinds of samples were produced, they were collected and tested at ambient temperature and pressure.

The crystal structure was analyzed by a powder x-ray diffraction (XRD) method at room temperature using Cu average x-ray wavelength radiation. The XRD patterns were indexed by using the reflex module combined in the Materials Studio program (Accelrys Inc.). The infrared absorption spectra were determined by Fourier transform infrared (FTIR) spectroscopy at room temperature. The electrical resistivity and carrier concentration data were obtained using AC Hall effect measurements with a constant magnetic field in the range ± 0.5 T and an electrical current ± 10 mA by a five-probe technique [18]. The carrier concentration was calculated from the Hall coefficient, assuming a single carrier model as a Hall scattering factor of unity. The voltage sensing electrodes and current electrodes were 50 μm diameter platinum wires which were mounted at the ends of the samples. The error in the measurement of the Hall coefficient and electrical resistivity is about 3%. The Seebeck coefficient was determined from thermoelectromotive force E_0 produced by the temperature difference within 2–3 K [18]. The error in the Seebeck coefficient does not exceed 5% at room temperature.

3. Results and discussion

XRD patterns of the samples synthesized at several typical conditions are shown in figure 2. The XRD patterns are the same as Kosuga's results [19]. It can be seen that the positions of the peaks do not change with synthesis pressure, and the positions of the peaks are the same as those of PbTe (for reference, see PDF # 381435). In order to get specific information from the XRD patterns, we indexed the XRD patterns of all the samples by using the reflex module included

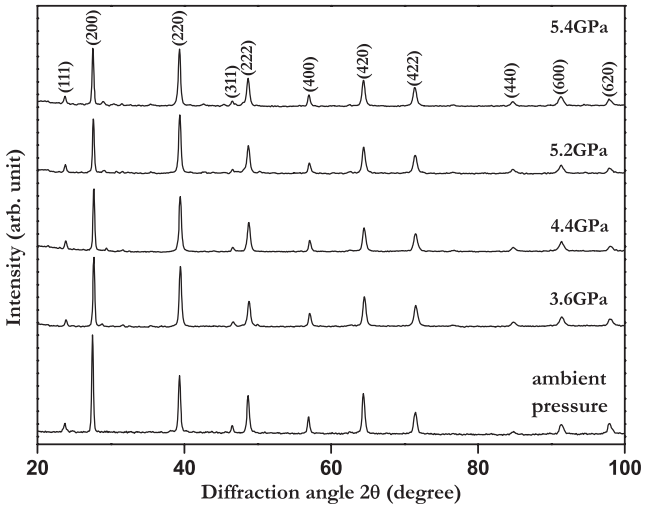

Figure 2. XRD patterns of samples synthesized at different pressure, measured at ambient temperature and pressure.

in the Materials Studio program. The peaks can be indexed unambiguously as those from a NaCl-type structure, and the space group is No. 225, $Fm\bar{3}m$. The Miller indices corresponding to the peaks are also shown in figure 2 in brackets. The cell parameters are shown in table 1. The cell parameter of the sample synthesized at ambient pressure is 6.459 ± 0.001 Å, which is the same as that obtained by Kosuga [19]. It is seen from table 1 that the cell parameters of the high-pressure synthesized samples are similar, apart from a small amount of fluctuation, and that they are a little larger than the ambient pressure one. In order to study the relation between the cell parameter and the synthesis pressure, we also investigated PbTe synthesized by HPHT, and performed XRD at ambient pressure. The *in situ* cell parameters of PbTe as a function of loading pressure were calculated using the full-potential linearized augmented plane-wave method within the density functional theory through the WIEN2K code [20]. The exchange–correlation potential was described with generalized gradient approximations (GGAs) and local density approximations (LDAs) with spin–orbit coupling. The Brillouin zone (BZ) integration was done with 72 k points in the irreducible part of the BZ. All the cell parameters are plotted in figure 3. The calculated ambient pressure cell parameters of PbTe were 6.5675 and 6.3922 Å for GGAs and LDAs respectively. The GGAs overestimate the equilibrium cell constant while the LDAs, in contrast, give smaller values. Our calculations of cell parameter at ambient pressure are similar to the calculations of Albanesi [21]. Although our calculations cannot give the exact cell parameters of PbTe under high pressure, the calculations can show the tendency of *in situ* cell parameters to change with loading pressure. It can be seen from figure 3 that compared to the cell parameters of high pressure *in situ* samples, the cell parameters of PbTe and $AgSbPb_{18}Te_{20}$ prepared by HPHT did not change obviously with the synthesis pressure, apart from some very small fluctuations.

The electrical resistivities and Seebeck coefficients of $AgSbPb_{18}Te_{20}$ versus synthesized pressure measured at ambient temperature and pressure are shown in figure 4. The electrical resistivity of the sample synthesized at ambient pressure is 1.374×10^{-3} Ω m. The electrical resistivity first decreases and then increases for the samples synthesized at 3.6 GPa and 4.4 GPa. Then there is a clear decrease of electrical resistivity for the sample synthesized at 5.2 GPa, and the electrical resistivity declines to its minimum value of 3.404×10^{-4} Ω m for the sample

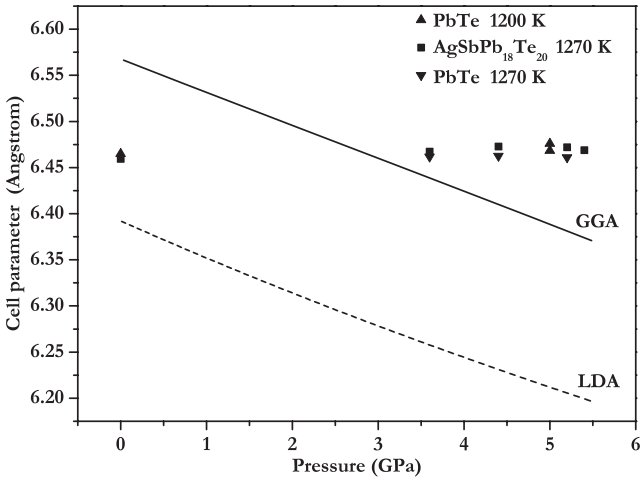

Figure 3. The cell parameters (tested at ambient temperature and pressure) versus synthesis pressure for $AgSbPb_{18}Te_{20}$ and PbTe prepared at HPHT and ambient pressure. The triangles show the cell parameters of PbTe synthesized at 0 and 5 GPa at 1200 K. (Cited from the doctoral dissertation of Gouzhong Ren, of our laboratory.) The squares show the cell parameters of $AgSbPb_{18}Te_{20}$ synthesized at different pressure at 1270 K. The inverted triangles show the cell parameters of PbTe synthesized at different pressure at 1270 K. The calculated *in situ* cell parameters of PbTe are also plotted as a function of loading pressure using the exchange–correlation potential of GGAs (the full line) and LDAs (the broken line).

Table 1. Cell parameters of the samples synthesized at different pressure, measured at ambient temperature and pressure.

Synthesis pressure (GPa)	Cell parameter (Å)
0	6.459 ± 0.001
3.6	6.467 ± 0.001
4.4	6.473 ± 0.001
5.2	6.472 ± 0.001
5.4	6.469 ± 0.001

synthesized at 5.4 GPa. This value of 3.404×10^{-4} Ω m is a quarter of the value for the sample synthesized at ambient pressure. There is a huge variation in Seebeck coefficient when the synthesis pressure changes from low to high. The Seebeck coefficient is 345.6 μV K^{-1} for the sample synthesized at ambient pressure, then it becomes increasingly smaller on increasing the synthesis pressure. Finally, the sign of the Seebeck coefficient reverses, and the p-type materials synthesized at 0, 3.6, and 4.4 GPa were changed into n-type materials as the synthesis pressure was raised to 5.2 and 5.4 GPa.

From the change of resistivity and Seebeck coefficients of $AgSbPb_{18}Te_{20}$, it can be seen that our $AgSbPb_{18}Te_{20}$ maintains the effects of HPHT synthesis. Our results are different from those of the *in situ* high-pressure experiments. For high-pressure *in situ* experiments, there are two cases. First, after the release of pressure, the electrical resistivity and Seebeck coefficient return to their ambient-pressure value [2–4]. This case can be explained as follows: when the lattice parameter returns to its value at ambient pressure, the resistivity and Seebeck coefficient return to their ambient-pressure value too. Second, when the pressure is loaded to a certain high level, there is hysteresis in the Seebeck coefficient after releasing the pressure to ambient pressure [2–4]. Meng [4] explained that the hysteresis was due to irreversible changes

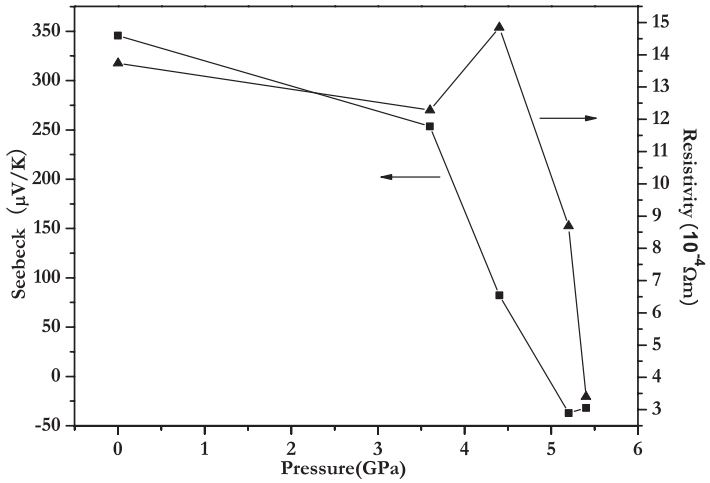

Figure 4. The resistivities and Seebeck coefficients versus synthesis pressure for $AgSbPb_{18}Te_{20}$ measured at ambient temperature and pressure. The squares represent the Seebeck coefficients, and the triangles represent the resistivities.

in crystallinity, defect concentration, etc, induced by compression to a certain pressure. So, regarding the influence of high pressure on the band structure, which determines the transport properties, there are two kinds of circumstance: one is that high pressure can change the distance between the atoms, and the other is that high pressure can help certain defects to be produced. Because there is no obvious change in the cell parameters of $AgSbPb_{18}Te_{20}$ synthesized under HPHT, it is the defects produced by HPHT that change the transport properties. The formation energy for a certain defect is likely to change under stress [22], which leads to a stress-dependent defect concentration. Quenching under high pressure may increase the formation of some certain defects. Since defects influence the electronic structure of the crystal, different electronic and transport properties can be expected after stress. Defects and or microstructural changes induced by compression may alter the proportion of p- and n-type carriers [2]. The sign reversal under high synthesis pressure suggests that both p- and n-type carriers can be tuned by defects produced by high pressure. Low pressure is helpful to produce acceptor defects and high pressure is helpful to produce donor defects.

In order to examine the microcosmic mechanism of the relation between the transport properties and the synthesis pressure, the Hall coefficient and carrier concentration were measured, and the results are listed in table 2. It can be seen from table 2 that up to a synthesis pressure of 4.4 GPa, the primary carrier is the hole. The hole concentration is 1.57×10^{23} m^{-3} for the sample synthesized at ambient pressure. Then the carrier concentration increases by one order of magnitude at the synthesis pressure of 3.6 GPa, and it decreases by one order of magnitude at 4.4 GPa compared to the value at 3.6 GPa. The primary carrier is the electron at the synthesis pressure of 5.2 and 5.4 GPa. The carrier concentrations of the n-type samples synthesized at 5.2 and 5.4 GPa are higher than that of the p-type sample synthesized at ambient pressure by two orders of magnitude. The different carrier concentrations in the samples synthesised under different pressures show that HPHT can change the type and amount of defects, and bring the defects to the ambient pressure. It is suggested from the Hall coefficients and carrier concentrations that low synthesis pressures favored producing acceptor defects, and high synthesis pressures favored producing donor defects. Different kinds and amounts of defects can alter the proportion of n- and p-type carriers and then alter the n- and p-type

Table 2. The Hall coefficients and carrier concentrations of the samples synthesized under different pressure, measured at ambient temperature and pressure.

Pressure (GPa)	Hall coefficient ($m^3\ C^{-1}$)	Carrier concentration (m^{-3})
0	$+3.98 \times 10^{-5}$	1.57×10^{23}
3.6	$+3.99 \times 10^{-6}$	1.56×10^{24}
4.4	$+4.11 \times 10^{-5}$	1.52×10^{23}
5.2	-9.57×10^{-8}	6.52×10^{25}
5.4	-9.49×10^{-8}	6.58×10^{25}

samples. The synthesis pressure of 4.4 GPa is a specific pressure value of transport properties and carrier concentration. The pressure zone in which the synthesis pressure of 4.4 GPa is may be a transition zone, in which the number of p-type carrier decreases and the number of n-type carriers increases. The low hole concentration can be regarded as being responsible for the high resistivity of the sample synthesized at 4.4 GPa. Some defects which provided the n-type carriers may be produced at 4.4 GPa, because the compensation of the holes by electrons favor the decrease of the p-type Seebeck coefficient.

The room-temperature infrared absorption spectra of $AgSbPb_{18}Te_{20}$ synthesized under different pressures are shown in figure 5. The unit for the X-axis was converted from wavenumber into electron volts in order to analyze the band structure conveniently. The curves shown in figure 5 for different synthesis pressures are dissimilar. The curve of the sample synthesized at ambient pressure is characterized by a sharp intrinsic absorption edge at about 0.064 eV; then the absorption slopes gently to the high-energy range. The curves for the samples synthesized at high pressure are characterized by a more gentle absorption edge. The absorption edges for samples synthesized at 3.6 and 4.4 GPa are near the minimum value of detection. But for the curves for samples synthesized at 5.2 and 5.4 GPa, the gentle absorption edge shifts to a higher energy level at about 0.091 and 0.093 eV, respectively. Before the intrinsic absorption edge there is a small absorption for the curves of the samples synthesized at ambient pressure, 5.2 and 5.4 GPa, respectively.

Since the band structures of $AgSbPb_{18}Te_{20}$ containing lattice defects synthesized under high pressure are not known to us, we can only obtain some useful information of band structure from the infrared absorption curves. Carrier absorption and localized state excitations (such as impurity and lattice imperfections) could be observed before the intrinsic infrared absorption edge [23]. So the absorption before the intrinsic absorption edge in the curves of samples synthesized at ambient pressure, 5.2 and 5.4 GPa, respectively, may be the carrier absorption or localized state excitations, or both. All the intrinsic absorption edges for the samples synthesized at high pressure became gentler than that of the sample synthesized at ambient pressure. It can be concluded that the density of states (DOS) at the bottom level of the conduction band of $AgSbPb_{18}Te_{20}$ synthesized under high pressure is smaller than that of the sample synthesized at ambient pressure. So the samples synthesized at high pressure have smaller degeneracy concentration in the bottom levels of the conduction band. The phenomena in our high-pressure synthesized samples are similar to those of n-type InSb [24]. InSb also possesses a small degeneracy concentration, so it becomes degenerate at relatively low electron densities. When the height of the Fermi level is above the bottom of the conduction band in n-type InSb, the Fermi level will increase very rapidly with increasing electron density. Then the absorption edge should shift with the Fermi level, and the absorption edge displaces with increasing carrier concentration in n-type InSb [24].

Here we can explain the reasons for the shift of the intrinsic absorption edge for our samples. Our samples are similar to n-type InSb [24–26]. HPHT synthesis increases the

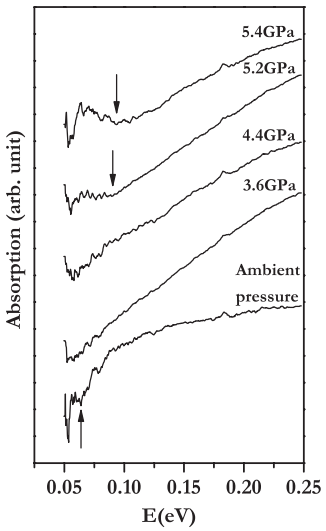

Figure 5. Infrared absorption spectra of $AgSbPb_{18}Te_{20}$ synthesized under different pressures, measured at ambient temperature and pressure. The synthesis pressure of each sample is listed beside the curves. For ambient synthesis pressure the absorption edge is about 0.064 eV, which is marked by arrows. For synthesis pressures of 5.2 and 5.4 GPa, the absorption edge shifts to a higher energy level at about 0.091 and 0.093 eV, respectively, which are marked by arrows.

concentration of the defects which supply the donors and then increases the concentration of n-type carriers. The Fermi energy is raised as the carrier concentration is increased, and eventually becomes higher than the bottom of the conduction band. For a small degeneracy concentration, the Fermi energy increases very rapidly with the increasing of carrier concentration in the conduction band. Below the Fermi energy, the energy bands are all filled with electrons. When the electrons in the top of valence band are excited by infrared rays to above the Fermi energy, it can be seen that the apparent band gap becomes larger. It is also clearly suggested that under the above circumstance the absorption limit shifts with the increase of carrier concentration. Usually this phenomenon can be seen for very high carrier concentration. For the samples synthesized at 5.2 and 5.4 GPa, the carrier concentrations are 6.52×10^{25} and 6.58×10^{25} m^{-3}, respectively, which are very high in semiconductors.

4. Conclusion

In summary, polycrystalline samples of $AgSbPb_{18}Te_{20}$ were synthesized at HPHT. The cell parameters did not change obviously with the synthesis pressure, apart from some small fluctuation. HPHT changed the kind and quantity of the defects, and changed the band structure of $AgSbPb_{18}Te_{20}$ accordingly. So the transport properties were changed by HPHT. The resistivity for the sample synthesized at 5.4 GPa was one quarter of that of the sample synthesized at ambient pressure. With increasing synthesis pressure, the Seebeck coefficients became increasingly smaller, and finally changed sign from positive to negative. The n-type carrier concentrations for the samples synthesized at 5.2 and 5.4 GPa were higher by two orders of magnitude than that of the p-type sample synthesized at ambient pressure. The pressure range in which the synthesis pressure of 4.4 GPa is can be regarded as a transition range in which the number of defects that produce acceptors and donors is decreased and increased, respectively. At high synthesis pressure the infrared absorption edge shifted to the high-energy

range. This was due to the small degeneracy concentration in the conduction band, and the absorption limit shifts with the increasing of carrier concentration.

HPHT might provide a method that could tune the kind and amount of defects, and eventually the band structure near the Fermi energy could be tuned. It might be fruitful to improve the performance of thermoelectric materials by tuning the concentration of defects through HPHT. We expect that excellent thermoelectric materials could be produced through HPHT synthesis in the future.

Acknowledgments

This work was supported by the National Basic Research Program of China (Grant no. 2001CB711201), the Key Research Program of Education Ministry of China (Grant no. 03057), the National Natural Science Foundation of China (Grant no. 50171030), and the 973 Program under grant no. 2005CB724400.

References

[1] Badding J V 1998 *Annu. Rev. Mater. Sci.* **28** 631
[2] Meng J F, Chandra Shekar N V, Badding J V, Chung D-Y and Kanatzidis M G 2001 *J. Appl. Phys.* **90** 2836
[3] Polvani D A, Meng J F, Chandra Shekar N V, Sharp J and Badding J V 2001 *Chem. Mater.* **13** 2068
[4] Meng J F, Polvani D A, Jones C D W, DiSalvo F J, Fei Y and Badding J V 2000 *Chem. Mater.* **12** 197
[5] Karolik A S and Sharando V I 2005 *J. Phys.: Condens. Matter* **17** 3567
[6] Huebener R P 1964 *Phys. Rev.* A **135** 1283
[7] Polak J 1964 *Czech. J. Phys.* B **14** 176
[8] Karolik A S, Lukhvich A A and Sharando V I 2004 *Fiz. Met. Metalloved.* **98** 1 (in Russian)
[9] Akulov N S, Lukhvich A A and Ljubyj V J 1973 *Fiz. Met. Metalloved.* **36** 303 (in Russian)
[10] Hsu K F, Loo S, Guo F, Chen W, Dyck J S, Uher C, Hogan T, Polychroniadis E K and Kanatzidis M G 2004 *Science* **303** 818
[11] Harman T C, Spears D L and Manfra M J 1996 *J. Electron. Mater.* **25** 1121
[12] Harman T C, Taylor P J, Walsh M P and LaForge B E 2002 *Science* **297** 2229
[13] Mahanti S D and Bilc D 2004 *J. Phys.: Condens. Matter* **16** S5277
[14] Zhu P W, Chen L X, Jia X, Ma H A, Ren G Z, Guo W L, Zhang W and Zou G T 2002 *J. Phys.: Condens. Matter* **14** 11185
[15] Zhu P W, Jia X, Chen H Y, Chen L X, Guo W L, Mei D L, Liu B B, Ma H A, Ren G Z and Zou G T 2002 *Chem. Phys. Lett.* **359** 89
[16] Ren G Z, Jia X P, Zhu P W, Zang C Y, Ma H A and Wang X C 2005 *Chin. Phys. Lett.* **22** 236
[17] Zhu P W, Jia X, Chen H Y, Guo W L, Chen L X, Li D M, Ma H A, Ren G Z and Zou G T 2002 *Solid State Commun.* **123** 43
[18] Uemura K and Nishida I A 1988 *Thermoelectric Semiconductors and their Applications* (Tokyo: Nikkan-Kogyo) pp 180–97
[19] Kosuga A, Kurosaki K, Uno M and Yamanaka S 2005 *J. Alloys Compounds* **386** 315
Kosuga A, Uno M, Kurosaki K and Yamanaka S 2005 *J. Alloys Compounds* **391** 288
[20] Blaha P, Schwarz K, Madsen G K H, Kvasnicka D and Luitz J 2001 *WIEN2k, An Augmented Plane Wave Plus Local Orbitals Program for Calculating Crystal Properties* (Austria: Vienna University of Technology) ISBN 3-9501031-1-2
[21] Albanesi E A, Okoye C M I and Petukhov A G 2000 *Phys. Rev.* B **61** 16589
[22] Thonhauser T, Jeon G S, Mahan G D and Sofo J O 2003 *Phys. Rev.* B **68** 205207
[23] Fan H Y 1956 *Rep. Prog. Phys.* **19** 107
[24] Burstein E 1954 *Phys. Rev.* **93** 632
[25] Kaiser W and Fan H Y 1955 *Phys. Rev.* **98** 966
[26] Tanenbaum M and Briggs H B 1953 *Phys. Rev.* **91** 1561